Two-photon excited hemoglobin fluorescence provides contrast mechanism for label-free imaging of microvasculature *in vivo*

Dong Li,[1,†] Wei Zheng,[1,†] Yan Zeng,[1] Yi Luo,[2] and Jianan Y. Qu[1,*]

[1]*Biomedical Engineering Program, Department of Electronic and Computer Engineering, Hong Kong University of Science and Technology, Hong Kong, China*

[2]*Bio_X Division, Hefei National Laboratory for Physical Science at the Microscale, University of Science and Technology of China, Hefei, Anhui 230026, China*

**Corresponding author: eequ@ust.hk*

Received December 13, 2010; revised January 16, 2011; accepted February 10, 2011; posted February 11, 2011 (Doc. ID 139575); published March 8, 2011

Direct visualization of microvasculature provides significant insights in microcirculation and critically impacts the diagnosis and treatment of microcirculatory diseases. Recently, we discovered that the high-energy Soret fluorescence of hemoglobin peaked at 438 nm with an extremely short lifetime becomes strongly visible under two-photon excitation. Based on the distinct spectral and temporal characteristics of hemoglobin fluorescence, we demonstrated that two-photon fluorescence microscopy could become a powerful tool for label-free *in vivo* imaging of microvasculature in tissue. © 2011 Optical Society of America

OCIS codes: 180.4315, 170.1470, 170.6935, 180.6900, 170.6920, 170.3880.

Microcirculation represents the smallest functional unit of the cardiovascular system and is a location where early manifestations of diseases can be encountered [1,2]. Physiological analysis of this system provides unique perspectives to the diagnosis and treatment of microcirculatory diseases that affect the microcirculation itself or the blood, including infection, diabetes, hypertension, ischemia, sickle cell disease, abnormal angiogenesis as in the case of cancer, etc. However, the well-established noninvasive imaging modalities, such as magnetic resonance imaging, computed tomography, positron emission tomography, ultrasound imaging, and Doppler optical coherence tomography, do not provide sufficient resolution to resolve the fine microvascular networks [3]. Two-photon microscopy has been adapted to produce three-dimensional (3D) volumetric visualization of the delicate feature of the microvasculature [4]. However, its imaging contrasts rely on exogenous fluorescent agents that may induce disturbance to the biological processes in the tissue and will face challenges from the strict regulations of clinical translations. Recently developed excited state absorption and stimulated emission microscopy took the advantage of the large absorption coefficient of hemoglobin and permit label-free 3D imaging of microvasculature with high sensitivity and resolution [5,6]. The pump–probe imaging methods require sophisticated excitation sources. Moreover, the signals of stimulated emission or excited state absorption could be interfered with by other chromophores of absorption spectra overlapping with hemoglobin. A subwavelength-resolution photoacoustic microscopy for *in vivo* vasculature imaging was demonstrated very recently [7]. The technique is also based on the absorption of hemoglobin.

Our recent discovery revealed that under short-wavelength two-photon excitation, hemoglobin emits strong high-energy Soret fluorescence peaked at 438 nm with an extremely short lifetime [8]. We found that the two-photon excitation efficiency in the wavelength region around 600 nm is significantly enhanced by near-resonance with the Q-band of hemoglobin (~560 nm). In addition, the two-photon excitation cross section of hemoglobin at 600 nm is comparable to tryptophan, which has been proven to be a good endogenous fluorescence agent for imaging of tissue [9,10]. In this Letter, we focus on *in vivo* imaging of microvasculature in tissue based on using the unique spectral and temporal characteristics of hemoglobin two-photon excited fluorescence (TPEF) signals excited at 600 nm. We demonstrate that the label-free *in vivo* imaging technique can obtain 3D structures of microvascular networks and even differentiate leukocytes from erythrocytes in the imaged capillary vessels.

The home-built two-photon microscope is similar to that reported in our previous study [8]. Briefly, the photonic crystal fiber was pumped by a femtosecond laser (Mira 900-F, Coherent, Inc., USA) tuned at 745 nm with a 76 MHz repetition rate. A portion of the pump laser of 250 fs pulse duration and a filtered-out supercontinuum at 600 ± 20 nm of 800 fs pulse duration were used as the excitation source. A water immersion objective lens with high UV to near-IR transmission (UAPO40XW3/340, 1.15NA, Olympus, Japan) was used to focus the excitation beams into the samples. A multichannel time-correlated single photon counting module (PML-16 and SPC-150, Becker & Hickl GmbH, Germany) was used as the detection system to provide the capability of time- and spectral-resolved measurements at each pixel of a TPEF image from 300 to 500 nm. The blood cells in the fresh blood sample were packed by spinning at 3000 rpm for 3 min and then washed with phosphate buffered saline (PBS) to remove the plasma. This procedure was repeated a few times to ensure that the plasma was completely removed. In the measurements, the blood cell suspension in PBS was put in a thin cuvette of two sides, made with microscope cover slips for imaging. The study of imaging microvasculature *in vivo* was conducted at the cheek pouch of a hamster under anesthesia. The image acquisition time for imaging blood cell samples and microvasculature in

hamster oral tissue was 8 s. For imaging individual blood cells in microvascular vessels *in vivo*, the image acquisition time was 1 s. The total power incident on the samples was less than 15 mW.

We first conducted the time- and spectral-resolved measurements from the blood cells. The color-coded TPEF images of blood cells and corresponding TPEF spectra and time decays are shown in Fig. 1. The color coding of the TPEF image was based on fluorescence emission wavelength or fluorescence decay time. In the display based on fluorescence wavelength, each pixel was assigned two independent colors. The fluorescence signals in the wavelength region from 300 to 400 nm, dominated by tryptophan, were displayed in cyan, whereas the signals in the region from 400 to 500 nm, dominated by hemoglobin fluorescence, were presented in red. In the display based on time decay, the pixels of a fluorescence decay time greater than and shorter than 300 ps were displayed in cyan and red, respectively. Both methods produced the same result of accurately separating the erythrocytes and leukocytes, as shown in Fig. 1(a). This could be further confirmed by integrating the spectral and time-decay signals from the cells colored in cyan and red, respectively. Figures 1(b) and 1(c) show that the TPEF spectrum and time-decay curves measured from cyan cells are consistent with the characteristics of tryptophan fluorescence, while the signals measured from red cells are almost identical to the hemoglobin fluorescence [8]. Therefore, the tryptophan and hemoglobin fluorescence could be completely differentiated from each other based on their spectral or lifetime characteristics.

Our previous study has shown that the TPEF signals in tissue excited at 600 nm are mainly tryptophan fluorescence peaked at 350 nm with a lifetime about 2.4 ns [9,10]. Therefore, it is possible to differentiate the TPEF signal of blood in microvasculature, which is dominated by hemoglobin fluorescence, from that of surrounding tissue based on the differences in the spectral line shape or lifetime of their TPEF signals. TPEF images at 600 nm excitation were measured from the hamster cheek pouch *in vivo*. The TPEF signals at each pixel of an image were recorded in the time and wavelength domains using time-resolved spectroscopic detection. Two simple algorithms were applied to process the TPEF signals and form the image to differentiate the microvasculature from surrounding tissue. First, we calculated the ratio of signal at each pixel in the wavelength band from 400 to 500 nm over the signal from 300 to 400 nm, where the hemoglobin and tryptophan signals were located, respectively. As shown in Fig. 2(a), by establishing an optimal threshold of ratio, image pixels with a ratio higher than the threshold were identified as microvasculature and labeled in red. As shown in Fig. 2(b), the TPEF spectrum integrated from the signals in the blood vessel consisted of both a tryptophan signal peaked around 350 nm and a hemoglobin signal peaked at 438 nm, making it distinct from the TPEF spectrum of the surrounding tissue, which only represented the tryptophan spectral characteristic. Because tryptophan fluorescence was not observed from the erythrocytes [8,11], its signal in blood must have been contributed from leukocytes and the dissolved proteins in plasma. This has been confirmed by analyzing the TPEF signals of plasma extracted from fresh blood (data not shown). In the second algorithm, we analyzed the time decay of the fluorescence signal at each pixel in the wavelength band from 300 to 500 nm to differentiate

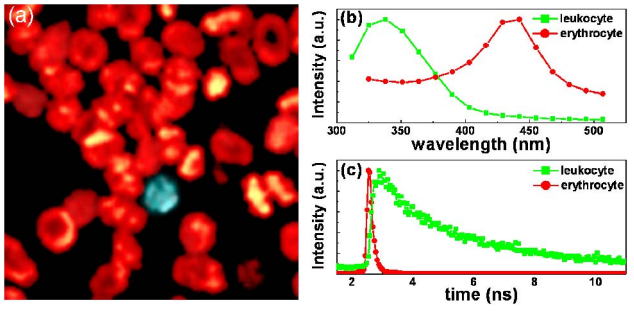

Fig. 1. (Color online) Images and fluorescence characteristics of blood cells at 600 nm excitation. (a) Color-coded TPEF image of blood cells with a leukocyte mixing with erythrocytes in PBS solution, (b) TPEF spectra of leukocyte and erythrocyte, (c) TPEF time-decay curves of leukocyte and erythrocyte. Image sampling area is 50 μm × 50 μm (128 pixels×128 pixels).

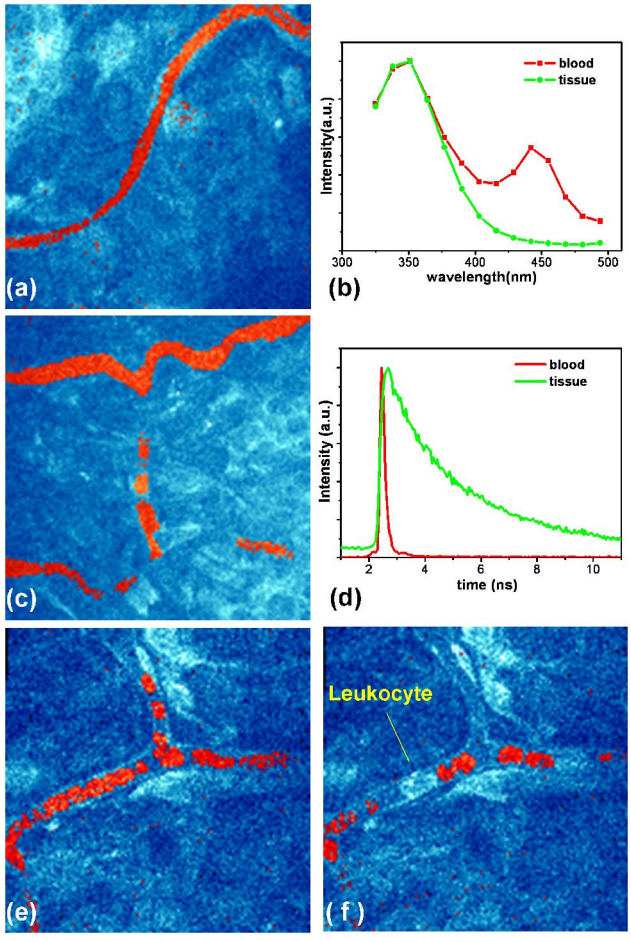

Fig. 2. (Color online) Representative TPEF images of microvasculature measured from hamster oral tissue *in vivo*. (a) Color-coded TPEF image of a microvascular vessel, (b) corresponding TPEF spectra of blood and surrounding tissue, (c) color-coded TPEF image of a microvascular vessel at a different location, (d) corresponding TPEF time decays of blood and surrounding tissue; (e) and (f) snapshots from blood cells movement video (Media 1): movements of (e) individual erythrocytes and (f) a leukocyte. Sampling area of each image (128 pixels ×128 pixels) is 100 μm × 100 μm.

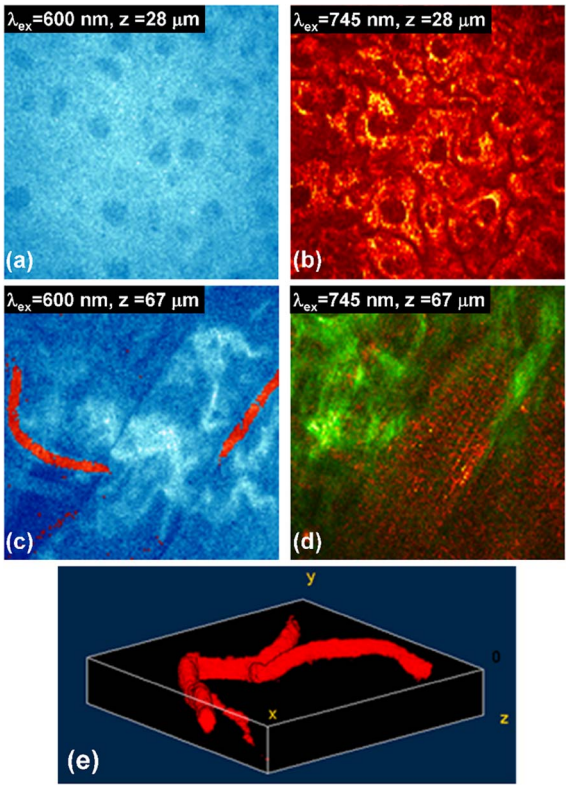

Fig. 3. (Color online) Multimodal TPEF images of hamster oral tissue *in vivo*. Tryptophan and hemoglobin signals excited at 600 nm are colored in cyan and red, respectively, and fluorescence and SHG signals excited at 745 nm are colored in red and green, respectively (detailed depth-resolved multimodal images are shown in Media 2). (a) and (b) Typical multimodal TPEF images from epithelial layer, (c) and (d) stromal layer, (e) 3D image of the microvascular networks reconstructed from depth-resolved TPEF images excited at 600 nm (see detail in Media 3). Sampling area of each image (128 pixels×128 pixels) is 100 μm × 100 μm.

the microvascular vessels from the surrounding tissue based on the extremely quick decay of hemoglobin fluorescence. To simplify the decay analysis, we calculated the ratio of the signal recorded in the first 300 ps to the signal recorded afterward. The results shown in Fig. 2(c) demonstrate that this fluorescence decay ratio algorithm also could identify the microvasculature accurately in the TPEF image by setting a threshold of ratio value. As shown in Fig. 2(d), the time-decay curve integrated from the signals in the blood vessel shows extreme quick decay that is a unique property of hemoglobin fluorescence [8], whereas the fluorescence integrated from the signals of the surrounding tissue exhibits the typical tryptophan fluorescence decay characteristic.

The highest image acquisition speed of the current system is one frame per second. To image individual blood cells in microvascular vessels, we slowed down the blood flow by gently pressing the tissue. Figure 2(e) shows that the individual erythrocytes were captured in a Y-shaped network. As shown in Fig. 2(f), a leukocyte-emitting tryptophan fluorescence was captured together with many other erythrocytes. The time-lapse movement of individual blood cells can be found in Media 1. The results demonstrate the potential of the imaging method for *in vivo* cytometry once the image acquisition is speeded up.

Moreover, we have combined the supercontinuum beam at 600 nm and the pump laser beam at 745 nm to simultaneously excite multiple nonlinear signals in tissue [10]. Based on the algorithm developed in this study, this simultaneous excitation allowed us to simultaneously image the microvasculature and the cellular structures of the surrounding tissue. Specifically, the supercontinuum was used to excite the TPEF signals of tryptophan and hemoglobin, while the 745 nm laser produced the second harmonic generation from collagen in stroma and myosin in soft muscle, and excited the TPEF signals of endogenous fluorophores in tissue, such as NADH, keratin, collagen, elastin, etc. Images of multiple two-photon nonlinear signals were acquired *in vivo* from the cheek pouch of a hamster by depth scanning at a depth interval of 1 μm. Rich structural and biochemical information of different tissue layers are obtained from the depth-resolved images [Fig. 3 (Media 2)]. As shown in Figs. 3(a) and 3(b), the images of tryptophan and NADH fluorescence reveal the cellular structures in the epithelial tissue layer. Figures 3(c) and 3(d) measured from the stromal layer display the microvascular and collagen networks, respectively. Here the stromal layer was identified by strong SHG signals generated from the collagen fiber. The microvasculature has been differentiated from the surrounding tissue using the fluorescence decay ratio method. Finally, a 3D structure of the microvascular network was extracted and reconstructed using the depth-resolved TPEF images excited at 600 nm. The 3D image of the microvasculature structure in the imaged tissue is shown in Fig. 3(e) and Media 3. As can be seen, microvascular vessels about the same size as an erythrocyte are clearly revealed.

We acknowledge support from the General Research Fund of the Hong Kong Research Grant Council (grant 618808) and the Hong Kong University of Science and the Hong Kong University of Science and Technology (grant RPC10EG33).

[†]These authors contributed equally to this work.

References

1. W. N. Durán, K. Ley, and R. F. Tuma, *Microcirculation* (Elsevier/Academic, 2008).
2. J. K. Li, *Dynamics of the Vascular System* (World Scientific, 2004).
3. D. M. McDonald and P. L. Choyke, National Library of Medicine current catalog proof sheets **9**, 713 (2003).
4. D. Kleinfeld, P. P. Mitra, F. Helmchen, and W. Denk, Proc. Natl. Acad. Sci. USA **95**, 15741 (1998).
5. D. Fu, T. Ye, T. E. Matthews, B. J. Chen, G. Yurtserver, and W. S. Warren, Opt. Lett. **32**, 2641 (2007).
6. W. Min, S. Lu, S. Chong, R. Roy, G. R. Holtom, and X. S. Xie, Nature **461**, 1105 (2009).
7. C. Zhang, K. Maslov, and L. V. Wang, Opt. Lett. **35**, 3195 (2010).
8. W. Zheng, D. Li, Y. Zeng, Y. Luo, and J. Y. Qu, Biomed. Opt. Express. **2**, 71 (2011).
9. D. Li, W. Zheng, and J. Y. Qu, Opt. Lett. **34**, 202 (2009).
10. D. Li, W. Zheng, and J. Y. Qu, Opt. Lett. **34**, 2853 (2009).
11. C. Li, R. K. Pastila, C. Pitsillides, J. M. Runnels, M. Puoris'haag, D. Cote, and C. P. Lin, Opt. Express **18**, 988 (2010).